Supplemental Information

Acetylation of yeast AMP-Activated Protein Kinase Controls Intrinsic Aging Independently of Caloric Restriction

Jin-Ying Lu,[1,2] Yu-Yi Lin,[3] Jin-Chuan Sheu,[4] June-Tai Wu,[5] Fang-Jen Lee,[5] Yue Chen,[6] Min-I Lin,[1] Fu-Tien Chiang,[1,4] Tong-Yuan Tai,[4] Shelley L. Berger,[7] Yingming Zhao,[6] Keh-Sung Tsai,[1,2,4] Heng Zhu,[8,10*] Lee-Ming Chuang,[2,4*] and Jef D. Boeke[9,10*]

[1]Department of Laboratory Medicine, National Taiwan University Hospital and [2]Graduate Institute of Clinical Medicine, [3]Institute of Biochemistry and Molecular Biology, College of Medicine, National Taiwan University, Taipei 100, Taiwan, [4]Department of Internal Medicine, National Taiwan University Hospital, [5]Institute of Molecular Medicine, College of Medicine, National Taiwan University, Taipei 100, Taiwan, [6] Ben May Department for Cancer Research, The University of Chicago, 929 East 57th Street, W421, Chicago, IL 60637, USA, [7]Gene Expression and Regulation Program, The Wistar Institute, Philadelphia, PA 19104, USA, [8]Department of Pharmacology and Molecular

Sciences, [9]Departments of Molecular Biology and Genetics, [10]The High Throughput Biology Center, The Johns Hopkins University School of Medicine, Baltimore, Maryland 21205

SUPPLEMENTAL FIGURE LEGENDS

Figure S1. Acetylated Lysine Residues K12, 16, 17 and 256 Were Identified by Tandem Mass Spectrometry, Related to Figure 1

(A-C) MS/MS spectra identified the following peptides: ^{Ac}K^{Deam}QTTK^{DiMe}K (A), QTT^{Ac}K^{DiMe}KCRAPI^{Ox}MSDVR (B), QTT^{Me}K^{Ac}KCR (C), QPE^{Me}KNPTNE^{Ac}KIRSK (D) in Sip2, with acetylation and other modifications. b and y ions represents fragment ions containing peptide N- and C-termini, respectively. Modified residues were underlined in the peptide sequence. "Ac" – acetylation, "Deam" – deamination, "DiMe" – dimethylation, "Me" – methylation, "Ox" – oxidation. All peptides were identified by Mascot 2.1 program (Matrix Science, London, UK) with cutoff $p<0.05$.

(D) Acetylation status of chromosomally integrated *sip2-K12R*, *sip2-K16R*, *sip2-K17R*, *sip2-K256R*, and *sip2-4KR in vivo*. *sip2-4KR*, *sip2-K12/16/17/256R*.

Figure S2. Enzyme Purification of Rpd3, Hda1 and Snf1, and Hda1 Activity, Related to Figure 1 and Figure 5

(A) The three TAP-tagged proteins were affinity purified as reported (Puig et al.,

2001) and each step of purification was monitored by immunoblots using a polyclonal anti-TAP (Open Biosystems, AB1001) antibody.

(B) The activity of purified Hda1-TAP was demonstrated by showing that it nearly totally deacetylated lysine 14 (K14) of FLAG-Htz1 purified from *hda1Δ* strain.

Figure S3. Isolation of Old Mother Cells; Measurement of Sip2 Acetylation in Various Carbon Sources, and Measurement of Intracellular Trehalose Levels in Low Glucose and Various Sip2 Acetylation Mutants, Related to Figure 3 and 4

(A) Endogenous Sip2-TAP protein levels were detected by immunoblots of whole cell extracts derived from cells expressing C-terminally TAP-tagged Sip2. Cells were grown in YEP (1% yeast extract, 2% peptone) media containing 2% glucose to mid-log phase, washed twice with YEP containing either 2% glucose (NG), 2% galactose (Gal), 0.05% glucose (LG), or 2% glycerol 3% ethanol (GE), and then grown in the same medium for another 2h. Acetylation species were determined by reverse immunoprecipitation using an anti-pan-acetyl-lysine antibody, and probed with an anti-TAP antibody.

(B) Relative abundance of Sip2 protein expression normalized to tubulin, and

relative Sip2 acetylation normalized to protein abundance were quantified and presented in bar graphs. Error bars indicate standard error of the mean (n=3). Statistical significance was assessed by one-way ANOVA with post-hoc test. *, $P < 0.05$; **, $P < 0.01$; ***, $P < 0.001$.

(C) Sorting of old cells (generation 7, G7) from young cells (generation 0, G0) was performed as described (Smeal et al., 1996) and an aliquot of sorted cells was stained with 100 µg/ml of Calcofluor White (Fluorescent Brightener 28, Sigma F3543) and visualized by a Zeiss Axioskop fluorescent microscope equipped with a Cool Snap FX camera.

(D) Trehalose levels were increased by carbon stress.

(E) The increased trehalose level of *esa1-531* was lowered by simultaneous *rpd3Δ* mutation.

(F) Both *sip2*-4KR and *sip2Δ* mutations furthered increased trehalose level in *rpd3Δ* cells. Error bars (B-D) show standard error of the mean (n=3).

Figure S4. Growth Curves and Cell Sizes of the *SIP2* Acetylation Mutants, Related to Figure 4

Cells from the indicated strains were grown from A_{600} ~0.1 to ~1.0. The growth curves are plotted with A_{600} on a log scale as a function of time in minutes. 95%

confidence intervals of the doubling time of each strain are shown in parentheses.

(A) The slower growth of *rpd3Δ* was partially rescued by simultaneous *sip2Δ* or *sip2-4KR* mutations.

(B) The *sip2-4KQ* grew more slowly than WT, *sip2Δ*, and *sip2-4KR*.

(C) Concomitant *sip2-4KQ* mutation significantly retarded the already slow growth of *esa1-531* cells at a semi-permissive temperature.

(D) Mean corpuscular volume (MCV) of various *SIP2* acetylation mutants were determined using a Z2 Coulter Counter (n=3 for each experiment). Data are presented with a box and whiskers plot to show the median, maximum, and minimum values.

Figure S5. Sch9 Phosphorylation Is Dependent on Sip2 Acetylation and Snf1 Kinase Activity, Related to Figure 5

(A) To verify the antibodies for immunoblotting were phosphorylation-specific, overexpressed GST-Sch9 was purified and treated with calf intestinal phosphatase (New England Biolabs, M0290S) with or without adding a phosphatase inhibitor Na_3VO_4 (Sigma-Aldrich, S6508). The phosphorylation signals were detected by immunoblotting and probed with phosphoserine and

phosphothreonine antibodies (Qiagen 37430 and 37420, respectively) following the manufacturer's protocol (Phospho-Protein Purification Handbook August, 2002; Qiagen).

(B) Protein ladder and uncropped gel images of endogenous Sch9-HA and no tag control, as well as those of Sch9-HA from WT and *snf1Δ* strains with and without rapamycin treatment were shown. Lysates were immunoprecipitated by anti-HA agarose and the phosphorylation signals of Sch9-HA were assessed by phosphoserine and phosphothreonine antibodies. The predicted size of Sch9-HA was about 131 kDa.

(C) Endogenous Sch9-HA was immunoprecipitated from *snf1Δ* strains supplemented with empty vector, wild type *SNF1* or kinase activity-abolished *snf1-K84R* constructs. The phosphorylation signal of Sch9-HA was assessed by phosphoserine and phosphothreonine antibodies.

(D) Overexpressed GST-Sch9 was purified from WT, *sip2Δ*, *sip2-4KR*, and *sip2-4KQ*, and the phosphorylation signal was assessed by phosphoserine and phosphothreonine antibodies.

(E) The slow growth pattern of *sch9Δ* was not affected by concomitant *sip2Δ* or *sip2-4KR* mutations.

Figure S6. Sch9 Is a Parallel Downstream Target of TORC1 and Sip2-SNF1, Related to Figure 6

(A) Comparison of growth patterns of WT, *rpd3Δ*, and concomitant *sip2-G2A rpd3Δ*, on YPD plate without and with rapamycin. Ten-fold dilutions of the above strains were spotted and grown on YPD without (2 days, 30^{o}C) or with rapamycin (25 ng/ml, 4 days, 30^{o}C).

(B) Comparison of replicative lifespan in WT cells with and without rapamycin (25 ng/ml, 30^{o}C).

(C) Comparison of replicative lifespan in *sip2-4KR* cells with and without rapamycin.

(D) Comparison of replicative lifespan in *sip2Δ* cells with and without rapamycin.

(E) Rapamycin (25 ng/ml) fails to further increase lifespan of *sip2-4KQ* and *rpd3Δ*.

(F) Snf1 kinase phosphorylates GST-Sch9 *in vitro* at sites other than T570 (one PDK phosphorylation site), S711, T723, S726, T737, S758 and S765 (six TORC1 phosphorylation sites) identified previously (Urban et al., 2007).

EXTENDED EXPERIMENTAL PROCEDURES

HPLC/MS/MS in an LTQ Mass Spectrometer

HPLC/MS/MS analysis was performed as described previously (Kim et al., 2006). The MS/MS spectra were acquired in a data–dependent mode that determined the masses of the parent ions and fragments of the ten strongest ions. If more than one spectrum were assigned to one peptide, each spectrum was given a Mascot score and only the spectrum with the highest score was used for fragmentation analysis. Peptides identified with a Mascot score higher than 25 were considered as potential positive identification and each of them was manually verified. The raw spectrum of each acetylated peptide was printed; a–, b–, y–type ions, their corresponding water/amine loss ions, and charge status were manually assigned. Strict manual analysis was applied to validate protein identification results using the criteria established earlier (Chen et al., 2005).

In vivo Acetylation

Acetylation signals were assessed as previously described (Lin et al., 2009). In brief, total cell lysates containing endogenous Sip2-TAP derived from WT,

esa1-531, *esa1-531 rpd3Δ*, and the *SIP2* acetylation mutants (*sip2-K12R*, *sip2-K16R*, *sip2-K17R*, *sip2-K256R*, *sip2-3KR*, *sip2-4KR*, *sip2-3KR rpd3Δ*, *sip2-4KR rpd3Δ*) were collected, pre-cleared by incubating with 30 µl protein A-sepharose beads at 4°C for 90 min, followed by immunoprecipitation by incubating with 30 µl protein A-sepharose beads (GE Healthcare) conjugated with 6 µl of mouse monoclonal anti-acetylated-lysine (Cell Signaling) in the presence of a cocktail of HDAC inhibitors (100 mM Trichostatin A, 50 mM nicotinamide, and 50 mM sodium butyrate) at 4°C for 3 hr. After extensive wash with 500 µl of washing buffer (50 mM HEPES [pH 7.0] and 100 mM NaCl) at 4°C four times (10 min each time), the beads was eluted by boiling in 20 µl of 2X SDS sample buffer, resolved by 4-20% Tris-Glycine SDS-PAGE (Invitrogen), transferred to nitrocellulose membranes using iBlot (Invitrogen) and probed with rabbit polyclonal anti-TAP antibody (Open Biosystems, AB1001).

Enzyme Purification and *In Vitro* Deacetylation Assays

Rpd3-TAP and Hda1-TAP were purified as described (Puig et al., 2001). About 5 µg of GST-Sip2 was subjected to ~0.5 µg of Rpd3-TAP or Hda1-TAP in deacetylation buffer (15 mM Tris-HCl pH7.0, 55 mM NaCl and 20 µM EDTA, 2

mM β-mercaptoethanol) with or without 100 μM of Trichostatin A (TSA) at 30°C for 1 h, and then immunoprecipitated by nProtein A Sepharose (GE healthcare) conjugated with anti-pan-acetyl-lysine monoclonal antibody (9681S; Cell Signaling) at 4°C for 3 h. After extensive washes (50 mM HEPES, pH 7.0, 100 mM NaCl) at 4°C for four times (10 min each time), beads were boiled in 20 μL 2XSDS (100 mM Tris-HCl, pH 6.8, 4% (w/v) SDS, 0.2% (w/v) bromophenol blue, 20% (v/v) glycerol) with 4% β-mercaptoethanol for 10 min. Eluted proteins were analyzed by immunoblotting using a rabbit polyclonal anti-GST antibody (Chemicon, AB3282).

Purification of FLAG-Htz1

The purification of FLAG-tagged Htz1p was performed as described (Lin et al., 2008; Luk et al., 2007). A CEN-plasmid containing *FLAG-HTZ1* was introduced into *hda1*Δ *htz1*Δ backgrounds and expressed as the sole source of the histone. WCEs were obtained by breaking cells from 0.5 L of cultures in exponential phase with zirconia/silica beads (BioSpec Products) in 5 ml of lysis buffer (100 mM Tris-HCl, pH 7.5, 150 mM NaCl, 1 mM EDTA, 1 mM EDTA, 10% v/v glycerol, 0.1% v/v Tween-20, 1 mM DTT, 1 mM PMSF, 5 μM pepstatin A, 1 μM MG-132, and EDTA-free complete protease inhibitor mix (Roche)).

FLAG-Htz1 was immunoprecipitated with the use of 200 µl of 50% M2 anti-FLAG agarose (Sigma, A2220), washed four times with wash buffer (20 mM Tris–HCl, pH 8.0, 100 mM KCl, 5 mM MgCl2, 0.2 mM EDTA, 10% glycerol, 0.1% Tween-20). Just prior to use, we added 10 mM 2-mercaptoethanol and 0.25 mM phenylmethylsulfonyl fluoride to wash buffer, and eluted the protein with 100 µl wash buffer containing 50 µg/ml 3X FLAG peptide (Sigma, F4799). The eluted protein was concentrated to a final concentration of 1.5 µg/µL by centrifugation through Vivaspin 500 concentration columns (Sartorius).

In Vitro Htz1 Deacetylase Assay

FLAG-Htz1 purified from *hda1*Δ*htz1*Δ cells was incubated with or without concentrated purified Hda1-TAP in deacetylation buffer (15 mM Tris-HCl pH7.0, 55 mM NaCl and 20 µM EDTA, 2 mM β-mercaptoethanol) at 30^{o}C for 1 hour. The samples were then denatured in boiling SDS sample buffer, resolved by SDS-PAGE, transferred to nitrocellulose membranes and probed with mouse monoclonal anti-FLAG (Sigma, F1804) and rabbit polyclonal anti-Htz1-K14^{Ac} (Millipore, 07-719) to assess the relative acetylation level of Htz1-K14.

Cell Size Determination

Cells are grown to a density of ~ $2x10^7$ per ml (A_{600} 1.0) and diluted 1:1,000 in 10 ml of Isoton II solution. Cell size was measured using Z2 Coulter Counter (Multisizer II; Beckman Coulter). Mean corpuscular volume of each strain was obtained from three independent experiments and presented with a box and whiskers plot to show the median, maximum, and minimum values.

In Vivo Sch9 Phosphorylation

GST-Sch9 was purified from WT, *sip2Δ*, *sip2-4KR*, and *sip2-4KQ* grown to mid-log phase with protein expression induced by adding 2% galactose as previously described (Lu et al., 2008). To suppress the TOR pathway phosphorylation, cells were treated with 200 ng/ml rapamycin (Sigma-Aldrich, R0395) for 30 min before collecting pellets. Phosphorylation signal of purified GST-Sch9 was assessed by immunoblotting using phosphoserine and phosphothreonine antibodies as described above. To determine the endogenous Sch9 phosphorylation status of WT *SNF1*, *snf1-K84R*, *snf1Δ*, and in young and old cells, cells expressing chromosomally-integrated *SCH9-HA* in the endogenous locus (to replace the *SCH9* gene) were either directly collected from various mutants, or sorted as young and old cells, and whole cell extracts were then immunoprecipitated by anti-HA sepharose (Santa-Cruz,

sc7392), followed by extensive washes (150 mM NaCl, 1% Triton X-100, 50 mM Tris-HCl pH7.6) at 4°C for four times (10 min each time), and eluted by boiling in 2X SDS sample buffer. The eluate was separated by SDS-PAGE and probed with phosphoserine and phosphothreonine antibodies as described above.

SUPPLEMENTAL REFERENCES

Chen, Y., Kwon, S.W., Kim, S.C., and Zhao, Y. (2005). Integrated approach for manual evaluation of peptides identified by searching protein sequence databases with tandem mass spectra. J Proteome Res *4*, 998-1005.

Kim, S.C., Sprung, R., Chen, Y., Xu, Y., Ball, H., Pei, J., Cheng, T., Kho, Y., Xiao, H., Xiao, L.*, et al.* (2006). Substrate and functional diversity of lysine acetylation revealed by a proteomics survey. Mol Cell *23*, 607-618.

Lin, Y.Y., Lu, J.Y., Zhang, J., Walter, W., Dang, W., Wan, J., Tao, S.C., Qian, J., Zhao, Y., Boeke, J.D.*, et al.* (2009). Protein acetylation microarray reveals that NuA4 controls key metabolic target regulating gluconeogenesis. Cell *136*, 1073-1084.

Lin, Y.Y., Qi, Y., Lu, J.Y., Pan, X., Yuan, D.S., Zhao, Y., Bader, J.S., and Boeke, J.D. (2008). A comprehensive synthetic genetic interaction network governing yeast histone acetylation and deacetylation. Genes Dev *22*, 2062-2074.

Lu, J.Y., Lin, Y.Y., Qian, J., Tao, S.C., Zhu, J., Pickart, C., and Zhu, H. (2008). Functional dissection of a HECT ubiquitin E3 ligase. Mol Cell Proteomics *7*, 35-45.

Luk, E., Vu, N.D., Patteson, K., Mizuguchi, G., Wu, W.H., Ranjan, A., Backus, J., Sen, S., Lewis, M., Bai, Y.*, et al.* (2007). Chz1, a nuclear chaperone for histone H2AZ. Mol Cell *25*, 357-368.

Puig, O., Caspary, F., Rigaut, G., Rutz, B., Bouveret, E., Bragado-Nilsson, E., Wilm, M., and Seraphin, B. (2001). The tandem affinity purification (TAP) method: a general procedure of protein complex purification. Methods *24*, 218-229.

Smeal, T., Claus, J., Kennedy, B., Cole, F., and Guarente, L. (1996). Loss of transcriptional silencing causes sterility in old mother cells of S. cerevisiae. Cell *84*, 633-642.

Urban, J., Soulard, A., Huber, A., Lippman, S., Mukhopadhyay, D., Deloche, O., Wanke, V., Anrather, D., Ammerer, G., Riezman, H.*, et al.* (2007). Sch9 is a major target of TORC1 in Saccharomyces cerevisiae. Mol Cell *26*, 663-674.

Supplementary Figure 1

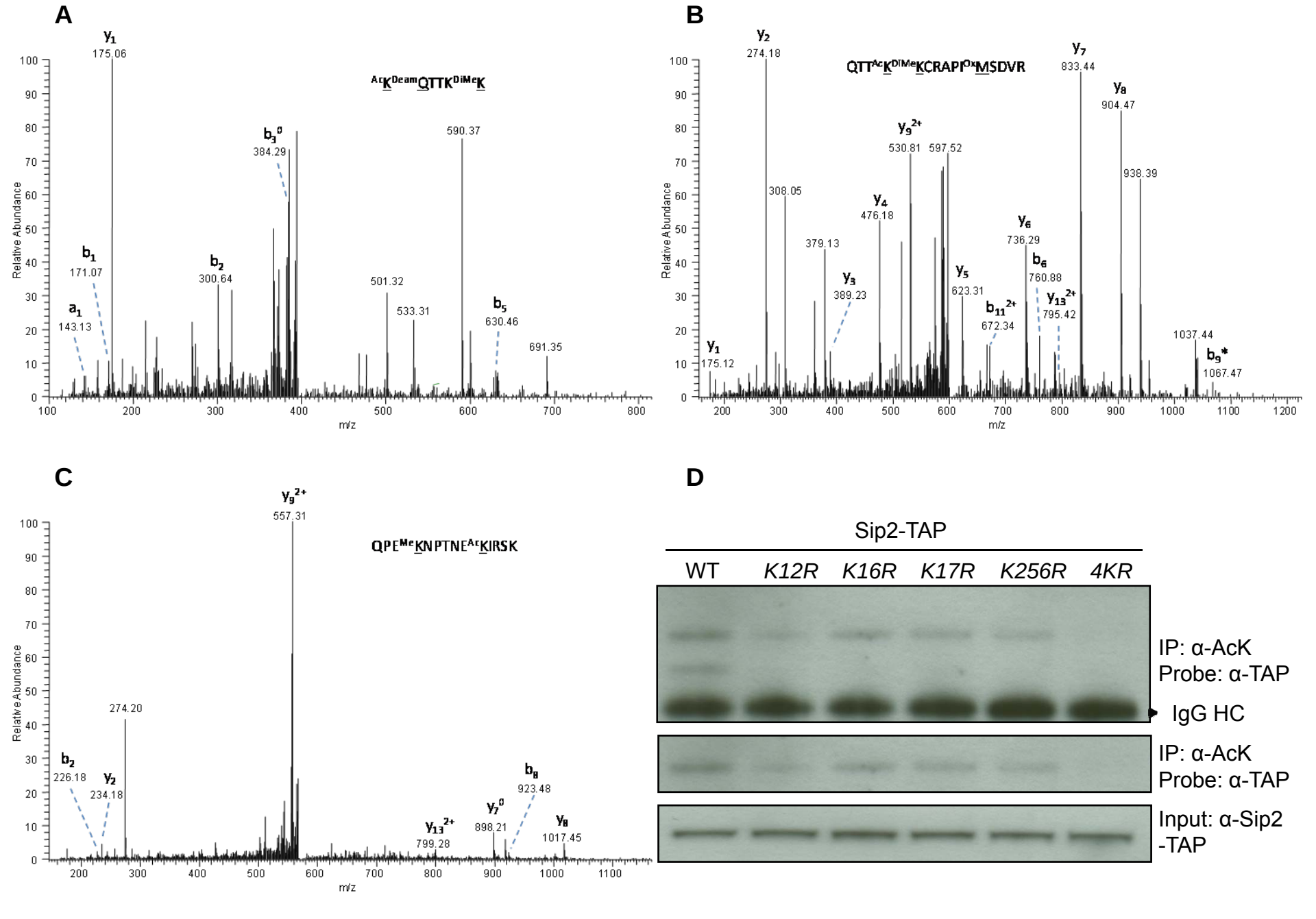

Supplementary Figure 2

A

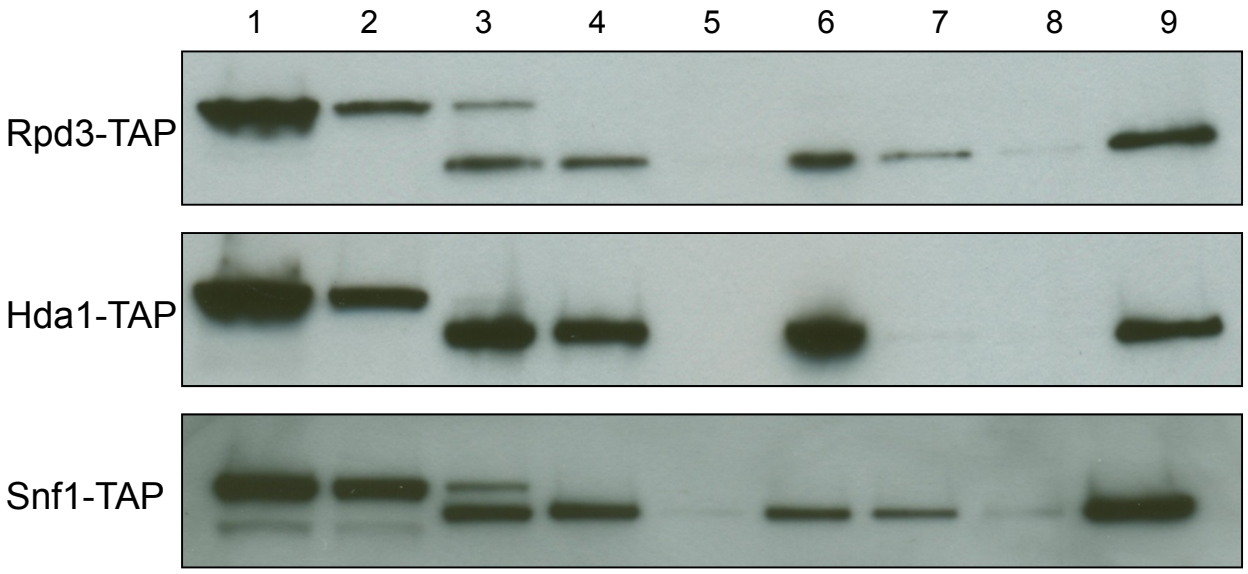

1. Whole cell extract
2. IgG supernatant after binding
3. IgG sepharose
4. TEV supernatant after cleavage
5. Calmodulin supernatant after binding
6. Calmodulin agarose
7. Elute 1
8. Elute 2
9. 20X concentrated protein

B

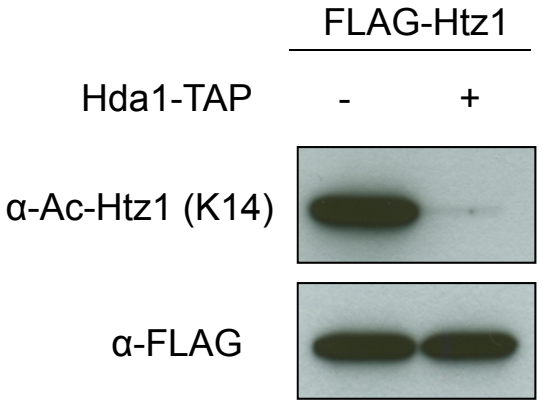

Supplementary Figure 3

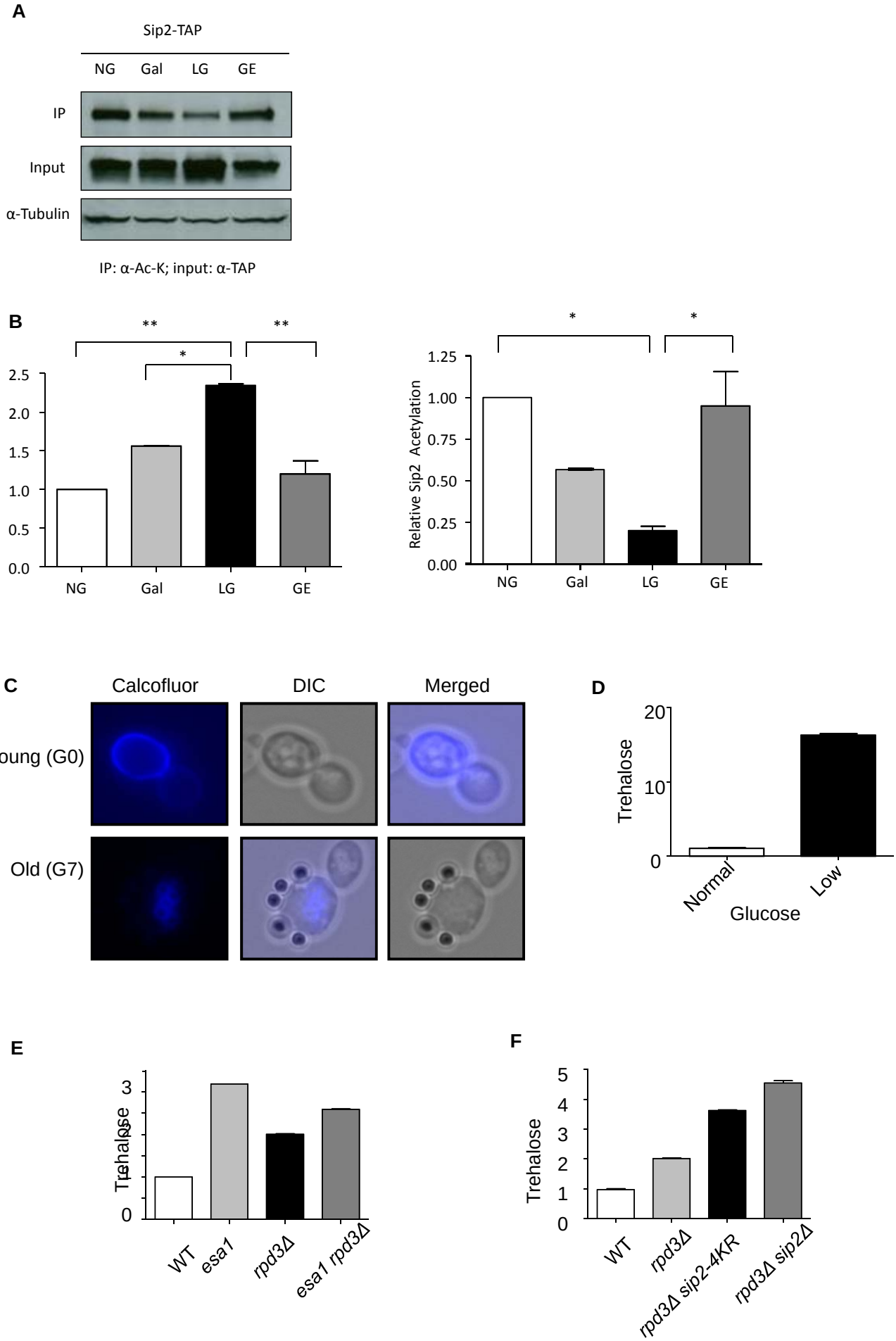

Supplementary Figure 4

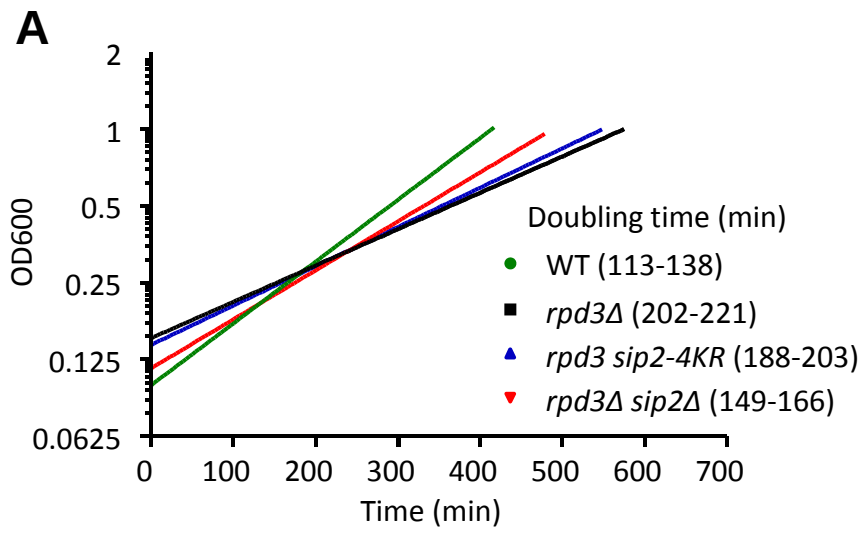

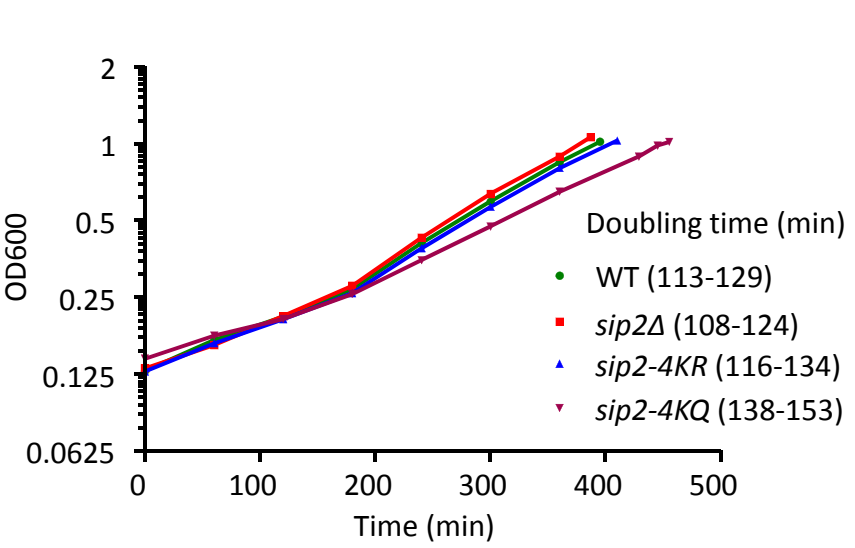

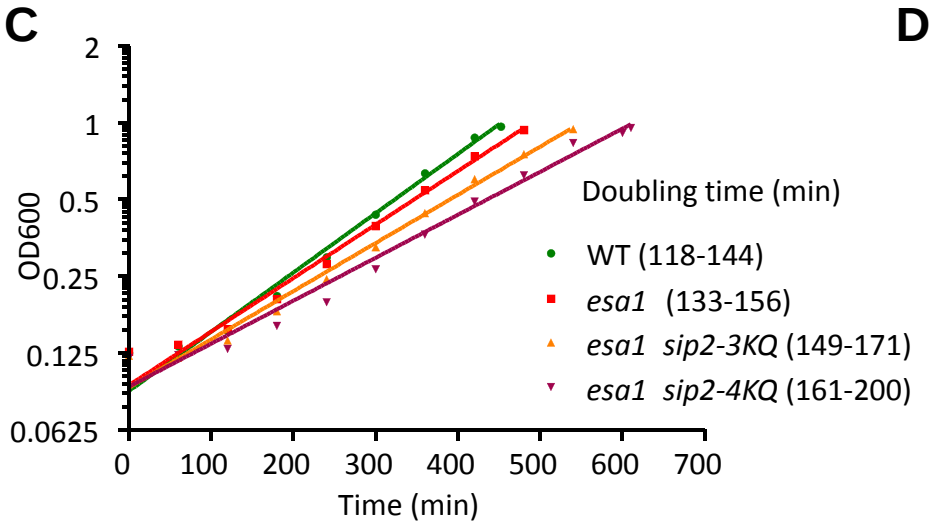

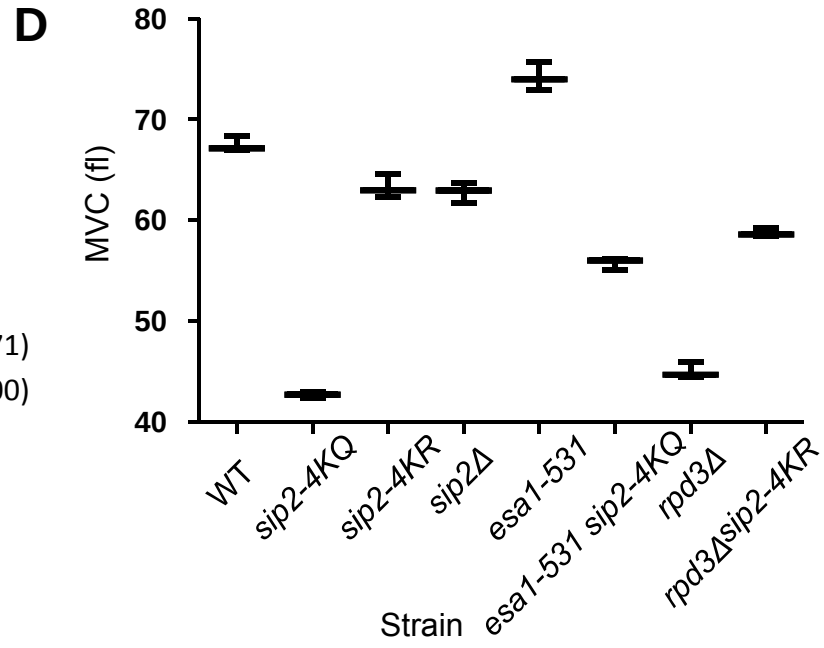

Supplementary Figure 5

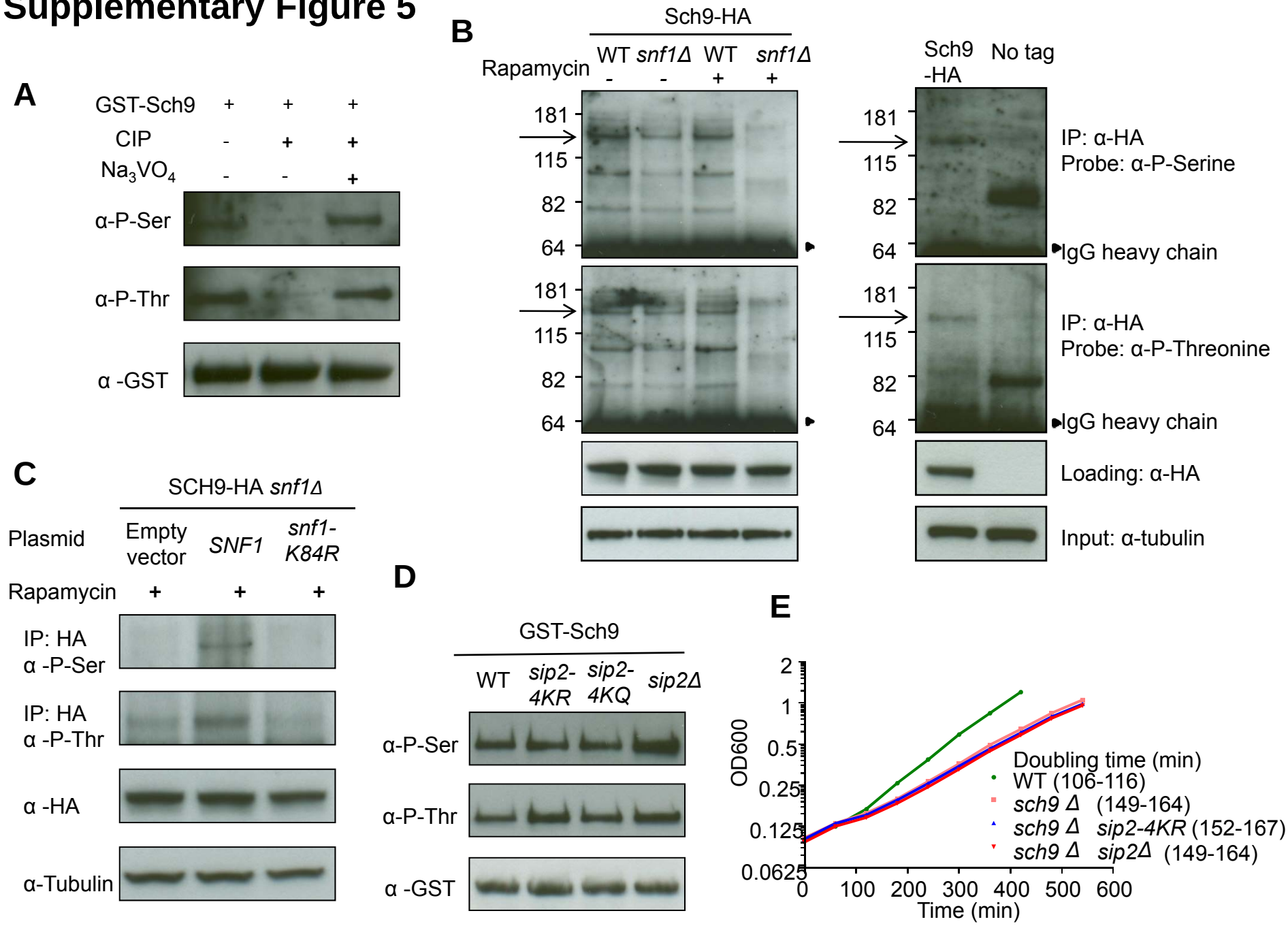

Supplementary Figure 6